

Functional Supramolecular Devices: $[M_4^{II}L_4]^{8+}$ $[2 \times 2]$ -Grid-Type Complexes as Multilevel Molecular Electronic Species

Mario Ruben,^[a, b] Esther Breuning,^[a] Mihail Barboiu,^[a] Jean-Paul Gisselbrecht,^{*,[c]} and Jean-Marie Lehn^{*,[a]}

Abstract: The $[M_4^{II}L_4]^{8+}$ $[2 \times 2]$ -grid-type complexes **1–8** present a set of features of particular interest for potential applications. All complexes exhibit multiple reduction levels at low reduction potentials paired with rather high stability. The modulation of the reduction potentials is possible by introduction of appropriate substituents on the ligands. The Co^{II}_4 complexes **1–5** present a remarkable regularity in the disposition of the reduction levels, indicating the ability of the Co^{II} sites to transmit electronic interactions between reduced ligands. In general, all investigated molecular systems **1–8** show characteristics typical for multilevel supramolecular electronic devices.

Keywords: cyclic voltammetry · N ligands · supramolecular chemistry · UV/Vis spectroscopy

Introduction

Fundamental physical constraints as well as economics are expected to limit continued miniaturization in electronics by conventional top-down manufacturing during the next one to two decades.^[1] Bottom-up approaches to electronics, in which the functional electronic structures are assembled from well-defined nanoscale building blocks, such as carbon nanotubes,^[2] semiconducting nanowires^[3] and/or molecules,^[4] have the potential to go far beyond the limits of conventional manufacturing. Of particular interest and great potential are approaches based on self-assembly processes capable of generating functional supramolecular devices by spontaneous but controlled build-up from their components, thus bypassing tedious nanofabrication and nanomanipulation procedures.^[5]

Scaling down electronic processes to the molecular level raises the question of controlling electron distribution in

molecules. Multistability on the molecular level, as required for high-density information storage devices on the nanoscale, might be achieved by exploitation of changes in intrinsic molecular properties, such as the redox state. Multicenter transition-metal complexes with different redox states appear to be very attractive candidates for the design of multilevel electronic devices.^[6]

The redox chemistry of polynuclear oligopyridine complexes has been investigated extensively and was reviewed recently.^[7] Most electrochemical studies deal predominantly with metal–metal interactions mediated through a bridging ligand. Rather few papers provide a detailed analysis of reduction processes,^[8] which may carry a wealth of information regarding the electronic interactions taking place in complexes, mainly between ligand-based redox centers. Such interactions among electrons localized on ligands are expected to be of the same order of magnitude as those between metal centers (at least, if the ligands are bound to the same metal center). Their detailed analysis opens the way to a better understanding of these multielectron species as potential components of metallo-supramolecular electronic devices. A prerequisite consists in the accurate determination of the localization of electronic changes in the individual redox steps.

Gridlike tetranuclear $[M_4^{II}L_4]^{8+}$ metal complexes with four octahedral coordination centers are accessible by self-assembly of a transition-metal ion and an appropriate bis-tridentate organic ligand in solution.^[9] Such $[2 \times 2]$ -grid species with $M = Co^{II}$ or Fe^{II} exhibit interesting magnetic behavior.^[10] In addition, Co_4^{II} complexes have been shown to present unique electrochemical properties.^[9a, 11] Related features are found in

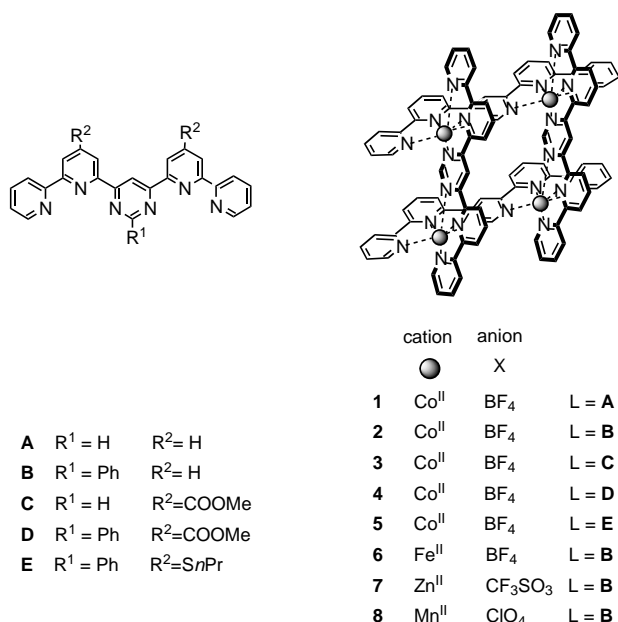
[a] Prof. J.-M. Lehn, Dr. M. Ruben, Dr. E. Breuning, Dr. M. Barboiu
ISIS-ULP-CNRS UMR-7006
4 rue Blaise Pascal, 67000 Strasbourg (France)
Fax: (+33) 3-90-24-11-17
E-mail: lehn@chimie.u-strasbg.fr

[b] Dr. M. Ruben
Institut für Nanotechnologie
Forschungszentrum Karlsruhe GmbH
PF 3640 76021 Karlsruhe (Germany)

[c] Dr. J.-P. Gisselbrecht
Laboratoire d'Electrochimie
et de Chimie-Physique du Corps Solide
UMR 7512, CNRS-Université Louis Pasteur
4, rue Blaise Pascal, 67000 Strasbourg (France)

a $[2 \times 2]$ -grid-type compound based on four tetrahedral Cu^I sites.^[12]

The $[M_4^{\text{II}}L_4]^{8+}$ $[2 \times 2]$ -grid-type complexes **1–8** (Scheme 1) were generated by self-assembly from the corresponding metal salt and ligand in acetonitrile solution. Their NMR and mass spectroscopic properties were in agreement with their structure following the characterizations described earlier.^[9] The products obtained could be used directly for the electrochemical investigations without further purification.



Scheme 1. Structure of the ligands **A–E** (left) and of the $[2 \times 2]$ grid-type complexes **1–8** (right).

A first series of five $[Co_4^{\text{II}}L_4][BF_4]_8$ complexes (**1–5**), involving variation of ligand **L**, was investigated to reveal the influence of ligand substitutions on the electrochemical behavior.

The influence of the nature of the metal ion on the electrochemical properties was studied by means of a second series of four complexes $[M_4^{\text{II}}L_4][X]_8$ keeping the same ligand **L = B**, but varying the metal ion: $[Co_4^{\text{II}}B_4][BF_4]_8$ (**2**),

Abstract in French: Une série de complexes **1–8** de type grille $[2 \times 2]$, $[M_4^{\text{II}}L_4]X_8$ (avec $M = Mn, Fe, Co, Zn$; $L = A–E$, $X = BF_4^-, ClO_4^-, CF_3SO_3^-$) a été synthétisée et leurs propriétés électrochimiques et spectro-électrochimiques ont été étudiées. Tous ces complexes présentent des réductions monoélectroniques multiples localisées sur les ligands et sont stables à la réduction. Les potentiels de réduction peuvent être modifiés par le choix de la nature des substituents. Les complexes du Co^{II} **1–5** possèdent des niveaux de réduction également espacés mettant en évidence l'aptitude de ces ions à transmettre l'interaction électrochimique entre les ligands. L'ensemble de ces propriétés donne aux complexes **1–8** le caractère de dispositifs fonctionnels supramoléculaires à niveaux électroniques multiples.

$[Fe_4^{\text{II}}B_4][BF_4]_8$ (**6**), $[Zn_4^{\text{II}}B_4][CF_3SO_3]_8$ (**7**), and $[Mn_4^{\text{II}}B_4][ClO_4]_8$ (**8**).

We present here an extended investigation of the electrochemical behavior of these grid-like $[M_4^{\text{II}}L_4]^{8+}$ complexes **1–8** incorporating differently substituted ligands **L** and various first row transition metal ions M^{II} . In addition, spectroelectrochemical experiments have been performed to confirm the assignment of the redox sites.

Results

Electrochemical reduction of $[M_4^{\text{II}}L_4][X]_8$ complexes **1–8**:

The electrochemical behavior of complexes $[M_4^{\text{II}}L_4][X]_8$ **1–8** ($M^{\text{II}} = Co, Fe, Zn, Mn$; $L = A, B, C, D, \text{ or } E$; $X = BF_4^-, CF_3SO_3^-, ClO_4^-$) was investigated in dimethylformamide (DMF) and acetonitrile (ACN) by cyclic (CV) and steady-state voltammetry on a glassy carbon disc electrode.

An extended sweep width over a large potential range was only accessible in DMF. However, in this solvent, slow decomposition by decomplexation within hours or minutes could be observed for several compounds by UV-visible spectroscopy. For this reason, all electrochemical studies were carried out only on freshly prepared solutions in a range of concentration of 5×10^{-4} M.

In ACN, no decomplexation was observed, neither during electrochemical studies nor by UV-visible spectroscopy. Indeed, the complexes have been proved to be more stable in this solvent. However, the low solubility of the electrochemically generated reduced species prevented investigations at more negative potentials.

Variation of the ligand **L**—Complexes **1–5**:

All Co_4^{II} complexes **1–5** in DMF give rise to seven well-resolved reduction waves during steady-state voltammetry in the available potential range. Analysis of the amplitude and of the log-plot slope indicates that the first reduction always presents the characteristics of two overlapping reversible one-electron reductions separated by 40 to 80 mV. In contrast, all following waves are well-separated, reversible one-electron transfers (log-plot slope for each step close to 60 mV, as expected for a reversible one-electron transfer).

Cyclovoltammetry of complexes $[Co_4^{\text{II}}L_4][BF_4]_8$ **1–5** in DMF at room temperature reveals well-resolved, multiple single-electron processes with complete reversibility for each compound (Table 1). Closer inspection of the redox potentials of complexes **1–5** in DMF exhibits, within the given similarity, a slight dependence of the electrochemical behavior on the ligand substitutions.

The CV of complex $[Co_4^{\text{II}}A_4][BF_4]_8$ (**1**) exhibits nine one-electron reduction steps at room temperature. In comparison, the reduction of $[Co_4^{\text{II}}B_4][BF_4]_8$ (**2**) under identical conditions leads to the same number of reduction steps, but with the first reduction potential slightly shifted to more positive values ($\Delta E_{1/2} = +60$ mV). Thus, substitution of the proton by a phenyl group in the 2-position of the pyrimidine causes a positive shift of the first reduction potential. However, this shift is less pronounced in the following reductions and was rather unexpected on the basis of the known inductive effects

Table 1. Redox potential E of the $[\text{Co}_4^{\text{II}}\text{L}_4][\text{BF}_4]_8$ complexes **1–5** in dimethylformamide (DMF) or acetonitrile (ACN) (0.1M Bu_4NPF_6 , glassy carbon electrode, versus Fc^+/Fc).

Reduction step	Complex						
	1 DMF	1 ACN	2 DMF	2 ACN	3 DMF	4 DMF	5 DMF
1	-0.65	-0.54	-0.59	-0.50	-0.45	-0.43	-0.65
2	-0.71	-0.58	-0.63	-0.58	-0.50	-0.47	-0.69
3	-0.92	-0.68	-0.78	-0.76	-0.63	-0.60	-0.82
4	-1.31	-0.90	-1.02	-1.01	-0.75	-0.82	-1.02
5	-1.57	-1.29	-1.32	-1.36	-1.03	-1.10	-1.37
6	-1.82	-1.55	-1.60	-1.61	-1.24	-1.30	-1.57
7	-2.04	-1.77 ^[a]	-1.85	-1.76 ^[a]	-1.45	-1.50	-1.82
8	-2.26		-2.11		-1.62	-1.70	-1.95
9	-2.40		-2.40		-1.89	-1.92	-2.07
10			-2.61 ^[b]		-2.05	-2.12	-2.32
11			-2.73 ^[b]		-2.12		
12					-2.20		

[a] Irreversible reduction: cathodic peak potential. [b] At -20°C .

of the substituents. Decreasing the temperature to -20°C resulted in an enlargement of the available potential window, thus giving rise to two additional reduction steps close to the electrolyte discharge.

The introduction of two electron-attracting ester groups per ligand into the 4'-position yields complex $[\text{Co}_4^{\text{II}}\text{C}_4][\text{BF}_4]_8$ (**3**), which bears a total of eight ester groups. The CV of **3** displays a very pronounced shift of the first reduction potential (Figure 1 top; $\Delta E_{1/2} = +200$ mV). This shift is even larger for the subsequent reduction steps and is increasing from step to step (all values relative to complex **1**). The complex $[\text{Co}_4^{\text{II}}\text{D}_4][\text{BF}_4]_8$ (**4**) bears both substitutions, a phenyl ring on the pyrimidine unit and the carboxymethyl groups in the 4'-position of the ligand. This leads to an even larger positive shift of the first reduction potential ($\Delta E_{1/2} = +220$ mV relative to **1**, Figure 1 bottom). On introduction of thio-*n*-propyl groups into the 4'-position of the ligands in $[\text{Co}_4^{\text{II}}\text{E}_4][\text{BF}_4]_8$ (**5**), the reduction potentials are close to those of the unsubstituted compound **1**. Apparently, the electronic influences of the four phenyl and the eight thio-*n*-propyl groups compensate each other in **5**, resulting in an electronic situation very similar to that of the reference compound **1**.

In ACN, complexes **1** and **2** give rise to a maximum of only seven reduction steps, whereas sharp peaks were observed on the reverse scan, whose shapes are characteristic for anodic redissolution processes. Evidently, the more reduced species are no longer soluble in ACN and precipitate on the electrode surface. However, CV in ACN carried out only to the sixth one-electron reduction give curves corresponding to well-resolved, reversible electron exchange. For completeness, the values for compounds **1** and **2** obtained in ACN are also given in Table 1.

Variation of the metal ion M^{II} —Complexes **2, 6–8:** In a second series, the electrochemistry of four complexes $[\text{M}_4^{\text{II}}\text{B}_4][\text{X}]_8$ **2, 6–8** containing different first-row transition-metal ions (with $\text{M} = \text{Co}^{\text{II}}, \text{Fe}^{\text{II}}, \text{Zn}^{\text{II}},$ and Mn^{II} , $\text{X} = \text{BF}_4^-, \text{ClO}_4^-,$ or CF_3SO_3^-) and the ligand **B** was investigated (Table 2). The Fe_4^{II} and Zn_4^{II} compounds **6** and **7** turned out to be less stable in DMF than the corresponding Co_4^{II} compound **2**; however, the first CV scan allowed the correct determination of the redox potentials

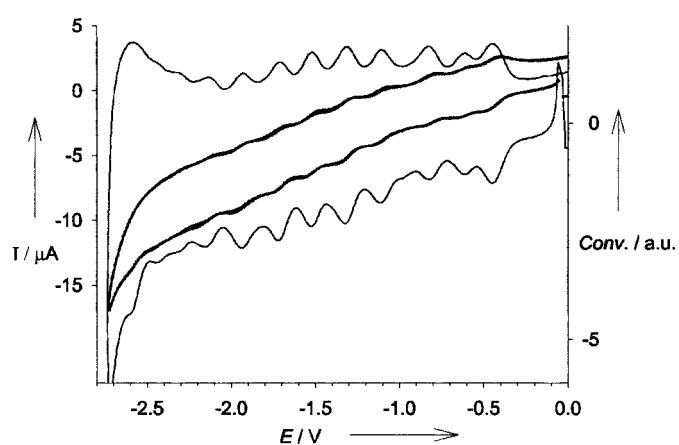
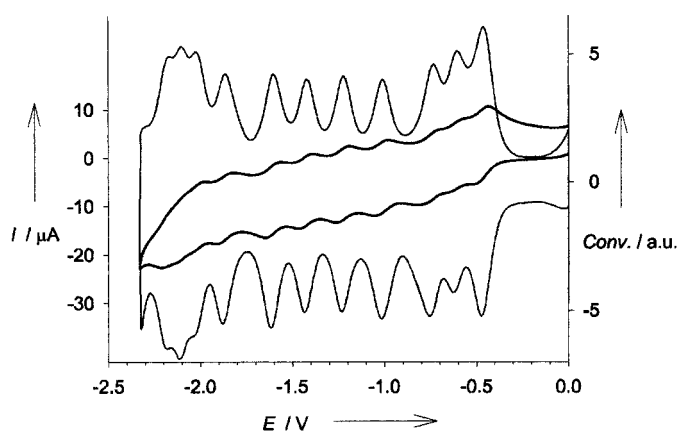


Figure 1. Cyclic voltammetry (bold: scan rate = 0.1 V s^{-1}) and its semi-derivative deconvolution (thin) of $[\text{Co}_4^{\text{II}}\text{C}_4]^{8+}$ (top) and $[\text{Co}_4^{\text{II}}\text{D}_4]^{8+}$ (bottom) in DMF + 0.1M Bu_4NPF_6 (potentials given versus ferrocene).

Table 2. Redox potential E of the $[\text{M}_4^{\text{II}}\text{B}_4][\text{X}]_8$ complexes **2** and **6–8** in dimethylformamide (DMF) or acetonitrile (ACN) (0.1M Bu_4NPF_6 , glassy carbon electrode, versus Fc^+/Fc).

Reduction step	Complex							
	2 DMF	2 ACN	6 DMF	6 ACN	7 DMF	7 ACN	8 DMF	8 ACN
1	-0.59	-0.50	-0.60	-0.53	-0.67	-0.60	— ^[c]	-0.60
2	-0.63	-0.58	-0.65	-0.57	-0.72	-0.68	— ^[c]	-0.68
3	-0.78	-0.76	-0.77	-0.70	-0.87	-0.83	— ^[c]	-0.82
4	-1.02	-1.01	-0.85	-0.80	-0.92	-0.91	— ^[c]	-0.92
5	-1.32	-1.36	-1.45	-1.29	-1.51	-1.36	— ^[c]	-1.57
6	-1.60	-1.61	-1.55	-1.40	-1.60	-1.51	— ^[c]	-1.67
7	-1.85	-1.76 ^[b]	-1.75	-1.50 ^[b]	-1.78	-1.61 ^[b]	— ^[c]	-1.82 ^[b]
8	-2.11		-1.89		-1.91			
9	-2.40		-2.45		-2.50			
10	-2.61 ^[a]		-2.60 ^[b]		-2.65			
11	-2.73 ^[a]							

[a] Irreversible reduction: cathodic peak potential. [b] Adsorption peaks. [c] Decomposition.

despite the presence of free ligand (arrows in Figure 2), resulting from partial decomplexation (Figure 2 top and bottom). In contrast, complex $[\text{Mn}_4^{\text{II}}\text{B}_4](\text{ClO}_4)_8$ (**8**) decomposed completely in DMF exhibiting only the reduction peak of the decomplexed ligand ($E_{1/2} = -1.95$ V). The use of ACN

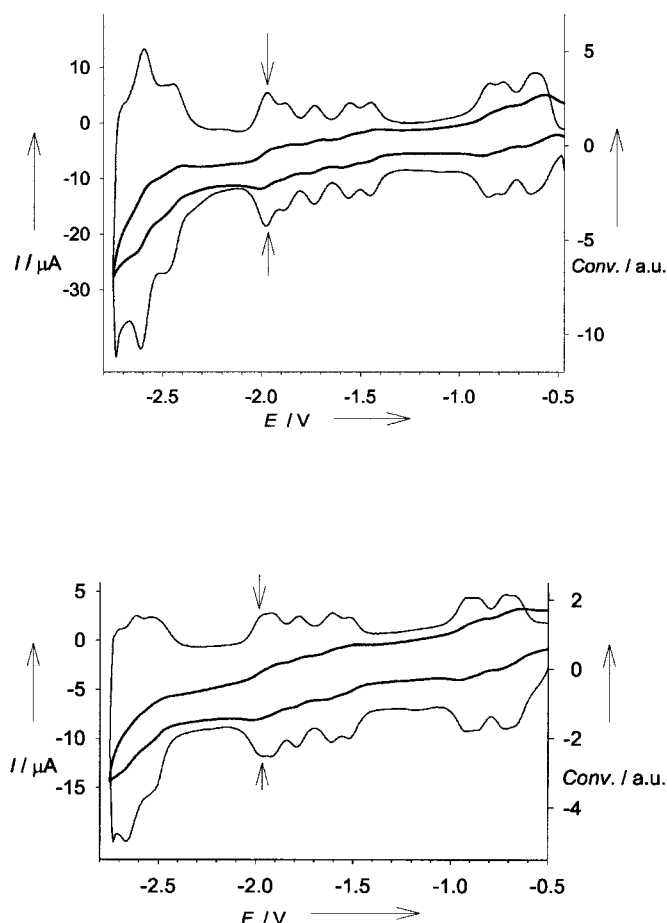


Figure 2. Cyclic voltammetry (bold: scan rate = 0.1 V s^{-1}) and its semi-derivative deconvolution (thin) of $[\text{Fe}_4^{\text{II}}\text{B}_4]^{8+}$ (top) and $[\text{Zn}_4^{\text{II}}\text{B}_4]^{8+}$ (bottom) in DMF + $0.1 \text{ M Bu}_4\text{NPF}_6$ (potentials given versus ferrocene; arrows indicate reduction of free ligand resulting from partial decomposition).

allowed the correct determination of the redox potentials of this compound in the restricted potential range as already described before for this solvent. Because of the stability problems within this series, all reduction potentials of complexes **6–8** are also given for the more stabilizing solvent ACN (Table 2). Similarly to compounds **1–5**, the CVs of complexes **6–8** provide multiple one-electron reduction schemes with complete reversibility of all observed reduction waves. Thus, $[\text{Fe}_4^{\text{II}}\text{B}_4][\text{BF}_4]_8$ (**6**) in DMF exhibits nine reversible reduction waves; however, they are not equally distributed over the potential range as observed for the Co^{II} complexes **1–5** (Figure 2 top). After the first set of four reductions with an internal wave separation of a maximum of $\Delta E_{1/2} = 120 \text{ mV}$, the onset of the second set occurs only after a potential shift of $\Delta E_{1/2} = 600 \text{ mV}$. Equally, after the second set of one-electron reductions, the third one starts only after a potential shift of around $\Delta E_{1/2} = 500 \text{ mV}$, but now the following reductions are disturbed by electrolyte discharge processes.

Because of the nonreducibility of its metal centers, the complex $[\text{Zn}_4^{\text{II}}\text{B}_4][\text{CF}_3\text{SO}_3]_8$ (**7**) constitutes an especially interesting variation within the series (Figure 2 bottom). It presents a redox behavior very similar to that found for the Fe_4^{II} complex **6**. One may conclude that the observed

reductions take place at the same redox sites in both complexes. Also, the corresponding Mn_4^{II} complex **8** exhibits a comparable CV in the restricted potential range of ACN with clustering of the reduction waves as found for **6** and **7**.

Spectro-electrochemical investigations: The electrochemical results described above suggest that the electronic characteristics of the gridlike compound are dominated by the electrochemical properties of the ligands. To determine the location of the injected electrons, we carried out spectro-electrochemical investigations on complexes $[\text{Co}_4^{\text{II}}\text{B}_4][\text{BF}_4]_8$ (**2**) and $[\text{Fe}_4^{\text{II}}\text{B}_4][\text{BF}_4]_8$ (**6**).

The UV-visible spectra of **2** were observed progressively up to the seventh reduction step (Figure 3 top). The evolution of the spectra during the first four one-electron reductions shows the progressive appearance of two new bands with maxima at 550 nm and around 800 nm , the smaller one of which at 550 nm shows some structuring. Simultaneously, the initial $\pi-\pi^*$ band of the unreduced ligand **B** at 370 nm decreases. Further reduction beyond the fourth electron equivalent results in an increase of the intensity of the two new bands proportional to the number of accepted electrons. The observation of the reduction process beyond the seventh

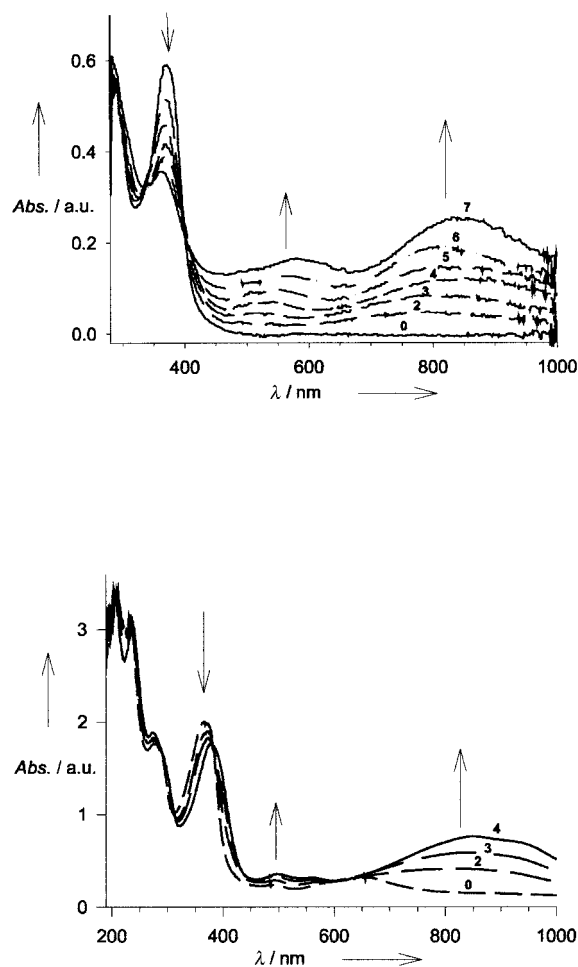


Figure 3. Time-resolved UV-visible spectra during stepwise reduction of $[\text{Co}_4^{\text{II}}\text{B}_4]^{8+}$ (top) in DMF + $0.1 \text{ M Bu}_4\text{NPF}_6$ for the six first reduction steps, and of $[\text{Fe}_4^{\text{II}}\text{B}_4]^{8+}$ (bottom) in CH_3CN + $0.1 \text{ M Bu}_4\text{NPF}_6$ for the four first reduction steps.

electron was not possible due to technical limitations of the experimental setup.

Because of its low stability in DMF, the complex **6** was investigated in ACN, restricting so the observation of reduction only up to the fourth electron. Once more, the striking feature of the spectrum obtained is the appearance of a broad low-energy band with a maximum at 846 nm, now covering the initial MLCT band of **6** at 662 nm. Simultaneously, a small structured band with two maxima at 497 and 565 nm emerges. At the same time, as found in **2**, the initial $\pi-\pi^*$ band of the unreduced ligand at 366 nm decreases and is shifted towards lower energies. The overall features of the reduction spectra in **6** resemble strongly those observed in the analogous Co_4^{II} compound **2**.

In both experiments, the initial spectrum could be regenerated quantitatively by stepwise reoxidation of the electro-generated reduced species (hepta-anion of **2** in DMF, tetra-anion of **6** in ACN). In view of the longer timescale of the spectro-electrochemical experiments, this is a remarkable indication for the absence of side reactions during the reduction of **2** and **6**.

Electrochemical oxidation of complexes 1–8: Under the present experimental conditions, none of the complexes **1–8** allowed the detection of well-defined oxidation steps by CV in DMF. Nevertheless, rotating disc voltammetry of **2** in ACN provides a long oxidation step corresponding to the transfer of four electrons at about +1.0 V. This step is widely spread out and has a log-plot slope of 300 mV. Such behavior is indicative of a kinetically slow process of the $\text{M}^{\text{III}}/\text{M}^{\text{II}}$ redox couple, occurring stepwise on the four metal ions of the complex. Slow electron-transfer rates seem to be inherent for encapsulated metal ions in bulky and dendrimeric structures and have been observed already in other systems.^[13, 14]

However, a previous investigation of complex $[\text{Co}_4^{\text{II}}\text{A}_4][\text{BF}_4]_8$ (**1**) with a different experimental setup (saturated calomel electrode (SCE) in DMF) exhibited analyzable oxidation signals.^[9a] Thus, compound **1** underwent a first oxidation at $E_{1/2} = +0.46$ V, followed by a two-electron oxidation at $E_{1/2} = +0.66$ V and by a fourth wave at $E_{1/2} = +0.91$ V (all values referred to SCE).

Discussion

Electrochemical features: The electrochemical experiments of both series (variation of either ligand L or metal ion M^{II}) resulted in multiple single-electron reduction processes exhibiting a good reversibility for all waves. The first series of complexes **1–5** shows that a systematic tuning of the first reduction potential is feasible by introduction of electron-donating or -attracting substituents on the ligand. The influence of each functional group can be evaluated qualitatively by comparing the first reduction potentials of complexes **1–5**. The phenyl group in the 2-position of the pyrimidine, although suffering a hindered conjugation with the rest of the ligand by intramolecular constraints,^[10b] acts still inductively as an electron-withdrawing substituent under these conditions and shifts the reductions of the complexes **2**

and **4** to more positive potentials ($\Delta E_{1/2} = +50$ to $+60$ mV). As expected, the ester group has the strongest effect on the first reduction potential ($\Delta E_{1/2} = +160$ to $+200$ mV), while the thio-*n*-propyl group leads only to a small shift towards more negative values. This behavior reflects basically the differences in their Hammett parameters of COOMe and thio-*n*-propyl groups ($\sigma_p = 0.45$ and 0.03).^[15]

The marked positive shift caused by the eight electron-attracting ester groups enables the observation of an increased number of reduction waves. Thus, reduction of complex **3** gives rise to twelve well-resolved one-electron waves even at room temperature. This represents the highest number of well-characterized, resolved and reversible one-electron reductions displayed by a molecular compound, reported so far. One may note that a tetranuclear $[2 \times 2]$ -grid-type Cu_4^{I} complex was found to have seven reduction potentials.^[12] Also, the fullerenes C_{60} and C_{70} exhibit six,^[16] the dinuclear compound $[\{\text{Ru}(\text{bpy})_2\}_2(\mu\text{-bpym})]^{4+}$ eight,^[8b] and the mononuclear $[\text{Ru}\{4,4'-(\text{EtOOC})_2\text{bpy}\}]^{2+}$ compound ten^[8c] reversible single-electron reductions in a comparable or larger potential window.

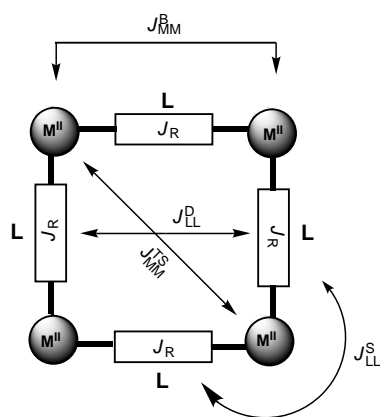
Within the second series (compounds **2, 6–8**), multiple one-electron reductions are observed as in the first series, but exhibiting a “clustering” of the reduction waves into sets of four reductions for $\text{M}^{\text{II}} = \text{Fe}^{\text{II}}, \text{Zn}^{\text{II}}, \text{Mn}^{\text{II}}$, in contrast to the regular change in potentials found for $\text{M}^{\text{II}} = \text{Co}^{\text{II}}$.

The similarity in number and pattern of the reduction steps in both series and the results of the UV-visible spectroscopic experiments (vide infra) are strong indications for ligand-centered reduction.

Compared with the mononuclear complexes $[\text{M}^{\text{II}}(\text{tpy})_2]^{2+}$,^[17, 18] the onset of the reduction processes of complexes **1–8** is strongly shifted towards positive values. This shift is in particular remarkable in complex **6**, whose first reduction potential is found at a 0.88 V more positive value than the complex $[\text{Fe}^{\text{II}}(\text{tpy})_2]^{2+}$ under similar experimental conditions. Since reductions at very low potentials represent a more easy access to and an enhanced stability of the reduced species, this electrochemical feature is of special importance for potential applicability of such species.

Scheme 2 represents the possible main electron repulsion interactions taking place in the symmetrical $[\text{M}_4\text{L}_4]$ species. J_{R} expresses the repulsive interaction between the reduction electron(s) on a given bridging ligand and the further incoming electrons. J_{LL}^{S} represents the interaction between the electrons located on ligands bound to the *same* metal center, whereas J_{LL}^{P} is the analogous interaction for parallel ligands bound to *different* metal ions and situated on opposite sides in the complex. J_{MM}^{R} and $J_{\text{MM}}^{\text{TS}}$ denote the interaction between the metal centers mediated through bridging ligands and occurring directly through space, respectively. These J values are not exactly accessible electrochemically, because only differences in half-wave potentials are measured experimentally. Nevertheless, the changes $\Delta E_{1/2}$ are roughly reflecting the changes in magnitudes of the repulsion terms.^[19]

The first two reduction waves of complexes **1–8** are always found in very close proximity, as consequence of the almost simultaneous reduction of two parallel ligands. $\Delta E_{1/2}$ values between the first and the second reduction ($\Delta E_{1/2} = 40-$



Scheme 2. Electronic interaction parameters in a $[2 \times 2]$ -grid-type complex. For definitions, see text.

80 mV) reflect rather small J_{LL}^D interactions. The electronic interactions mediated through one unreduced ligand and two interjacent metal centers seem to be similarly small for all investigated complexes.

In the case of the Fe_4^{II} , Zn_4^{II} , and Mn_4^{II} complexes **6–8**, the reduction waves are “clustered” into three sets of four reductions, with an internal spacing within the set of $\Delta E_{1/2} = 50\text{–}200$ mV and a potential shift of $\Delta E_{1/2} = 560\text{–}650$ mV between successive sets (Table 2, Figure 2). This is the behavior one may expect. Indeed, the first gap inserts between the fourth and the fifth reduction, where each of the four ligands has already accepted one electron, so that incoming electrons have to overcome the repulsive interaction J_R with the electron already present on the same ligand. This repulsion is normally reflected in the amount of spin-pairing energy in polypyridine ligands found to be about $\Delta E_{1/2} = 600\text{–}700$ mV.^[19]

In marked contrast, all Co_4^{II} complexes **1–5** show a regular spacing of $\Delta E_{1/2} = 130\text{–}390$ mV for all subsequent reductions occurring at ligands bound to the same metal ion as an already reduced ligand, (Table 1; Figure 1). This even spacing of the one-electron processes over the whole potential range is indicative of electronic communication J_{LL}^S between the ligand centered redox sites through the interjacent common Co^{II} ion. Remarkably, the J_R interaction appears to be decreased in these Co_4^{II} complexes relative to the others, and to have become similar in magnitude to J_{LL}^S . Closer inspection of the CVs indicates that there is nevertheless a limited potential shift ($\Delta E_{1/2} = 140\text{–}390$ mV) after each fourth reduction, noticeably smaller, however, than the 560–650 mV observed for complexes **6–8** containing no Co^{II} sites.

Evidently, the differences in the magnitude of the J_R interaction between the Co_4^{II} compounds **1–5** and the other complexes **6–8** reflect the ability of the interjacent M^{II} ions to mediate J_{LL}^S interactions (equally expressed by larger J_{LL}^S values for the Co_4^{II} compounds of $\Delta E_{1/2} = 130\text{–}390$ mV for **1–5** compared to $\Delta E_{1/2} = 50\text{–}200$ mV for **6–8**). A better mediating ability of the interjacent Co^{II} ions between the reduced ligand anions should lead to a certain electronic coupling over the complex, thus reducing the repulsion for incoming further electrons.

These features portray electronic interactions between ligand-centered redox sites mediated through “bridging metals”, in contrast to the well-investigated metal–metal interactions through “bridging ligands”.^[20]

The previously reported oxidation of compound $[\text{Co}_4^{\text{II}}\mathbf{A}_4][\text{BF}_4]_8$ (**1**) gives additional access to the metal–metal interactions J_{MM}^B and J_{MM}^{TS} .^[9a] The one-two-one sequence evokes a preference of successive oxidations of adjacently located Co^{II} centers. Consequently, the second two-electron step would represent the simultaneous oxidation of two diagonally situated Co^{II} ions expressing a through-space J_{MM}^{TS} interaction, which is apparently too small to be determined. On the other hand, the separation between the first and second two-electron steps and thereafter between the two-electron and the last oxidation step should represent the electronic J_{MM}^B interaction of two adjacent Co^{II} -ions through the bridging pyrimidine group of the ligand. Thus, the J_{MM}^B values of $\Delta E_{1/2} = 200$ and 250 mV indicate substantial electronic interaction between two adjacent metal centers, corresponding to a medium strong comproportionation constant of $K_{\text{com}} = 1.7\text{–}2.4 \times 10^3$.^[20]

Electronic spectra: Although carried out in different solvents, the spectral behavior of the Co_4^{II} complex **2** and of the Fe_4^{II} complex **6** during reduction is similar (Figure 3). As reduction proceeds, a broad spectral band around 800 nm and a smaller, more structured band around 550 nm emerge, while at the same time the band below 400 nm decreases progressively. Additionally, the MLCT transition around 620 nm in compound **6** disappears or is covered by the new bands. All changes in intensity occur almost linearly with the number of electrons added.

The two new emerging low-energy bands in **2** and **6** can be assigned, by comparison with the absorption spectra of the mono-reduced form of uncoordinated bipyrimidine (bpym) in DMF (two bands with $\lambda_{\text{max}} = 500$ and 800 nm) and of coordinated bipyrimidine in mono-reduced $[\text{Fe}(\text{bpym})_3]^{2+}$ (two bands with $\lambda_{\text{max}} = 510$ and 1020 nm), to intraligand $\pi^* - \pi^*$ transitions from the new SOMOs (mono-anion) to the first and the second new LUMOs (mono-anion) of the four monoreduced $\mathbf{B}^{\cdot-}$ radical anions.^[18, 21]

Interestingly, the emerging bands in the absorption spectra of **6** exhibit a linear increase in intensity of the radical bands (without any additional perturbations of the spectra) even beyond the fourth electron added. This is in line with the formation of a dianion \mathbf{B}^{2-} , similar to bpym^{2-} observed in the reduction of μ -bipyrimidine in $[\{\text{Ru}(\text{bpy})_2\}_2(\mu\text{-bpym})]^{4+}$.^[8c]

The band of the nonreduced ligand in **2** and **6** located below 400 nm can be assigned to the $\pi - \pi^*$ transition of the ligand **B**. Consequently, its intensity decreases on progressive population of the LUMO of the coordinated ligand by the reducing electrons.

It is worth mentioning that all intraligand reduction bands, increasing and decreasing, experience a subsequent shift to lower energies on progressive reduction, especially beyond the fourth reduction. This red shift can be associated with an electronic destabilization of the corresponding HOMOs of the ligands, as a consequence of the second electron introduced into the ligand orbitals.

No evidence for low-lying interligand and intervalence transitions has been found. Also, aggregate formation at the used concentrations (less than 5×10^{-4} M) can be excluded by the spectroscopic data.

Conclusion

The electrochemical behavior of the family of tetranuclear gridlike oligopyridine complexes **1–8** of the general formula $[M_4^{\text{II}}L_4]^{8+}$ displays well-resolved multiple one-electron reductions for all compounds independent of the nature of ligands **A–E** and of the coordinated metal ions M^{II} .

Introduction of electron-donating and -attracting groups into the ligands systematically tunes the potential of the first reduction. As a consequence, reduction of complex $[\text{Co}_4^{\text{II}}\mathbf{B}_4][\text{BF}_4]_8$ (**3**) exhibits up to twelve well-resolved reversible one-electron processes at room temperature; this appears to be the most extended redox series known for well-characterized molecular compounds.

The rather low values of the redox potentials are of importance for the stability of the generated multielectron species and thus for their possible applications as devices presenting multiple electronic levels. For the Co_4^{II} complexes the repulsive interaction parameter J_R is unusually small, and comparable to the electronic interaction J_{LL}^{S} between two neighboring ligands through an interjacent metal ion. Since J_R was found for the non- Co_4^{II} compounds in the expected range, this difference displays an ability of the Co^{II} ion (relative to Fe^{II} , Zn^{II} , and Mn^{II}) to better mediate electronic interactions. This is also confirmed by slightly larger J_{LL}^{S} values for all investigated Co_4^{II} complexes. Thus, the ability of different M^{II} ions to act as “bridging metals” for electronic interactions seems to be responsible for the differences in the pattern of the reduction scheme.

Spectro-electrochemical experiments revealed that the reductions take place on the coordinated organic ligands, independent of the nature of the metal ions involved. No indication for reduction of the metal centers was observed in the accessible potential range.

The oxidation of complex **1**^[9a] reveals a medium strong J_{MM}^{B} interaction between adjacent metal centers mediated by the pyrimidine groups of the ligands, while the electronic $J_{\text{MM}}^{\text{TS}}$ interaction between nonadjacent metal centers through space is too small to be determined.

Further study of the nature of the radical anions $L^{\cdot-}$ and of the dianions L^{2-} and their interplay with the different open spin-bearing metal ions (implicating even spin-crossover phenomena),^[10b] requires magnetic and EPR investigations of the reduced species.

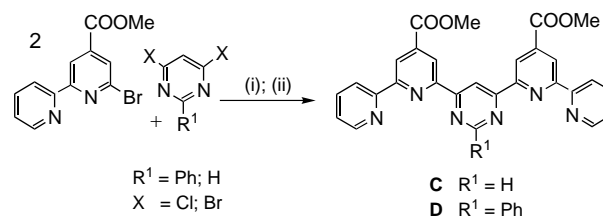
In conclusion, the grid-type complexes **1–8** present a set of features of particular interest for potential applications as supramolecular electronic devices: 1) multiple reduction levels, 2) ease of reduction, 3) stability towards reduction, 4) modulation of the reduction potentials by appropriate substituents on the ligands, and 5) in the case of the Co^{II} species, regularity in disposition of the reduction levels.

Experimental Section

Electrochemistry: The electrochemical studies were carried out on 5.10^{-4} M solutions of complexes **1–8** in DMF + 0.1 M Bu_4NPF_6 or in ACN + 0.1 M Bu_4NPF_6 in a classical three-electrode cell connected to a computerized electrochemical device AUTOLAB (Eco Chemie B.V. Holland). The working electrode was a glassy carbon disc (3 mm diameter), the auxiliary electrode a platinum wire, and the pseudoreference electrode a silver wire. The measurements were carried out by cyclic voltammetry and by steady-state voltammetry (rotating disc electrode). In our experimental conditions all potentials are referred versus ferrocene, used as an internal standard. DMF and acetonitrile (both Aldrich, spectroscopic grade) were dried over molecular sieves 4 Å prior to use. The measurements were carried out at room temperature and in some cases at -20°C . Spectro-electrochemical studies were carried out in a home made borosilicate glass cell with an optical pathway length of 0.1 mm placed in a diode array UV/Vis spectrophotometer HP8453 (Hewlett Packard). The OTTE cell was a platinum grid (1000 mesh) placed in the optical pathway. The auxiliary electrode was a platinum wire and the reference electrode was an aqueous Ag/AgCl electrode. Under the described experimental conditions, ferrocene, which was used as internal standard in all measurements, was oxidized at +0.45 V.

Synthesis: All reagents were obtained from commercial suppliers and used without further purification unless otherwise noted. The following solvents were distilled prior to use: tetrahydrofuran (THF) and diethyl ether from sodium and benzophenone, and dimethyl sulfoxide (DMSO) from calcium hydride under Ar. All organic solutions were routinely dried over magnesium sulfate or sodium and solvents were removed under vacuum using a rotary evaporator. ^1H and ^{13}C NMR spectra were recorded on a Bruker AC200 spectrometer at 200 MHz and 50 MHz, respectively. Flash chromatography was performed by using neutral alumina (activity 2). FAB mass spectra were performed on a Fisons TRIO-2000 (Manchester) and a Micromass AUTOSPEC-M-HF spectrometer using 3-nitrobenzoic alcohol as matrix. IR data were collected on Perkin-Elmer 1600 Series FTIR spectrometer. Microanalyses were carried out by the Service de Micro-analyse, Faculté de Chimie, Strasbourg. Melting points were measured on a digital electrothermal apparatus and are uncorrected.

Ligands: The synthesis of ligands **A** and **B** was described earlier.^[22, 10b] Ligands **C** and **D** were synthesized by using Stille-type coupling procedures following the reactions depicted in Scheme 3.



Scheme 3. i) Sn_2Me_6 , $[\text{Pd}(\text{PPh}_3)_4]$ (cat.); ii) $[\text{Pd}(\text{PPh}_3)_4]$ (cat.).

2-Bromo-4-(methylcarboxylate)-6-(pyrid-2'-yl)pyridine: 2-(Tributylstannyl)pyridine^[23] (672 mg, 1.83 mmol), 2,6-dibromo-4-(methylcarboxylate)pyridine^[24] (700 mg, 2.37 mmol), and $[\text{Pd}(\text{PPh}_3)_4]$ (137 mg, 0.19 mmol) were combined in toluene (10 mL), flushed with Ar, and heated under reflux for 39 h. The mixture was poured into KF (10 mL saturated solution) and, after addition of Et_2O , was stirred for 2 h. The precipitate was filtered and the phases were separated. The aqueous phase was extracted with Et_2O (2×40 mL). The combined organic phases were washed with H_2O (1×30 mL) and dried over MgSO_4 , and the solvent was evaporated. The product was purified by column chromatography on silica by using hexane/ EtOAc (3:1 v/v) as eluant to give 2-bromo-4-(methylcarboxylate)-6-(pyrid-2'-yl)pyridine as a white powder. Yield: 221 mg (0.75 mmol, 41 %); m.p. 142°C ; ^1H NMR (200 MHz, CDCl_3 , 298 K): $\delta = 3.99$ (s, 6H; CH_3), 7.36 (ddd, $J = 7.6, 4.9, 1.2$ Hz, 1H; H^2), 7.84 (td, $J = 7.9, 1.8$ Hz, 1H; H^4), 8.04 (d, $J = 1.2$ Hz, 1H; H^3 or H^5), 8.42 (dt, $J = 7.9, 1.2$ Hz, 1H; H^3), 8.70 (ddd, $J = 4.8, 1.8, 0.9$ Hz, 1H; H^6), 8.91 ppm (d, $J = 1.2$ Hz, 1H; H^3 or H^5); ^{13}C NMR (50 MHz, CDCl_3 , 298 K): $\delta = 52.8, 119.1, 121.4, 124.5, 127.2, 136.9, 140.6, 141.9, 149.2, 153.5, 158.1, 164.2$ ppm; EI-MS: m/z : 293.9 $[M^+]$, 233.9 $[M^+ -$

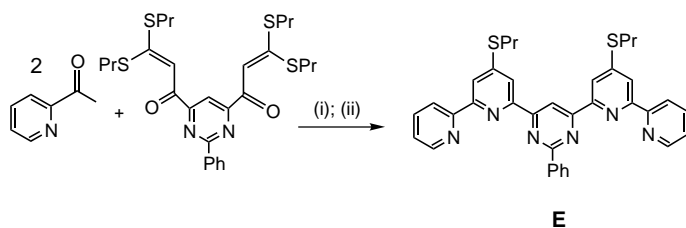
COOMe]; IR (KBr): $\tilde{\nu}$ = 3007, 2956, 1732, 1585, 1550, 1433, 1381, 1310, 1242, 1118, 994, 977, 813, 763, 731, 664 cm^{-1} ; elemental analysis calcd (%) for $\text{C}_{12}\text{H}_9\text{BrN}_2\text{O}_2$: C 49.17, H 3.09, N 9.56; found: C 49.43, H 3.41, N 9.20.

4,6-Bis[4'-(methylcarboxylate)-6'-(pyrid-2'-yl)pyrid-2'-yl]pyrimidine (Ligand C): 2-Bromo-4-(methylcarboxylate)-6-(pyrid-2'-yl)pyridine (211 mg, 0.72 mmol), hexamethyldistannane (259 mg, 0.79 mmol), and $[\text{Pd}(\text{PPh}_3)_4]$ (42 mg, 0.036 mmol) were combined in toluene (5 mL), flushed with Ar and heated under reflux for 30 min. The solvent was evaporated and the crude stannylated product was used for the following coupling reaction without further purification. ^1H NMR (200 MHz, CDCl_3 , 298 K): δ = 0.41 (s, 9H; $\text{Sn}(\text{CH}_3)_3$), 3.96 (s, 3H; CH_3), 7.81 (td, J = 7.9, 1.8 Hz, 1H; H^4), 8.00 (d, J = 1.5 Hz, 1H; H^3 or H^5), 8.54 (d, J = 7.9 Hz, 1H; H^3), 8.69 (d, J = 4.3 Hz, 1H; H^6), 8.79 ppm (d, J = 1.5 Hz, 1H; H^3 or H^5); FAB-MS (NBA): m/z : 379.2 $[M^+]$.

4-(Methylcarboxylate)-6-(pyrid-2'-yl)-2-(trimethylstannyl)pyridine (812 mg, 2.15 mmol) and 4,6-dibromopyrimidine (250 mg, 0.76 mmol) were combined in toluene (10 mL), degassed, and $[\text{Pd}(\text{PPh}_3)_4]$ (48 mg, 0.042 mmol) was added. The solution was flushed with Ar and heated under reflux for 24 h. The precipitate was filtered off, washed with MeOH and acetone and dried in vacuo to give **C** as an off-white powder. Yield: 350 mg (0.69 mmol, 91%); m.p. > 300 °C; ^1H NMR (200 MHz, $\text{CDCl}_3/\text{CF}_3\text{COOD}$, 298 K): δ = 4.11 (s, 6H; CH_3), 8.20 (t, J = 5.8 Hz, 2H; $\text{H}^{4''}$ or $\text{H}^{5''}$), 8.55 (d, J = 7.3 Hz, 2H; $\text{H}^{3''}$), 8.65 (t, J = 8.8 Hz, 2H; $\text{H}^{4''}$ or $\text{H}^{5''}$), 8.76 (d, J = 1.1 Hz, 2H; H^3 or H^5), 9.34 (d, J = 5.8 Hz, 2H; $\text{H}^{6''}$), 9.39 (d, J = 1.1 Hz, 2H; H^3 or H^5), 9.54 (d, J = 1.5 Hz, 1H; H^5), 9.94 ppm (d, J = 1.1 Hz, 1H; H^2); ^{13}C NMR (50 MHz, $\text{CDCl}_3/\text{CF}_3\text{COOD}$, 298 K): δ = 105.8, 111.4, 117.1, 122.8, 142.7, 143.3, 148.0, 159.5, 160.4, 161.2, 162.1, 163.9 ppm; FAB-MS: m/z : 505.1 $[M^+ + \text{H}]$; IR (KBr): $\tilde{\nu}$ = 1733, 1580, 1537, 1431, 1376, 1349, 1235, 1111, 1068, 761, 683 cm^{-1} ; elemental analysis calcd (%) for $\text{C}_{28}\text{H}_{20}\text{N}_6\text{O}_4$: C 66.66, H 4.00, N 16.66; found: C 66.62, H 3.72, N 16.68.

4,6-Bis[4'-(methylcarboxylate)-6'-(pyrid-2'-yl)pyrid-2'-yl]-2-phenylpyrimidine (Ligand D): 4-(Methylcarboxylate)-6-(pyrid-2'-yl)-2-(trimethylstannyl)pyridine (244 mg, 0.65 mmol), 4,6-dichloro-2-phenylpyrimidine (73 mg, 0.32 mmol), and $[\text{PdCl}_2(\text{PPh}_3)_2]$ (18 mg, 0.026 mmol) were combined in anhydrous DMF (5 mL), degassed, flushed with Ar, and heated to 100 °C for 46 h. The solvent was evaporated and the residue taken up in MeOH/acetone (1:1 v/v). The precipitate was centrifuged off, washed with MeOH/acetone, and dried in vacuo. The residue was dissolved in boiling CHCl_3 and filtered, and the solvent was evaporated to give ligand **D** as an off-white powder. Yield: 90 mg (0.16 mmol, 44% over 2 steps); m.p. > 250 °C (decomp); ^1H NMR (200 MHz, CDCl_3 , 298 K): δ = 4.09 (s, 6H; CH_3), 7.39 (dd, J = 6.4, 4.9 Hz, 2H; $\text{H}^{5''}$), 7.60–7.63 (m, 3H; H^{meta} and H^{para}), 7.91 (td, J = 6.7, 1.5 Hz, 2H; $\text{H}^{4''}$), 8.75–8.86 (m, 6H; H^{ortho} , $\text{H}^{3''}$ and $\text{H}^{6''}$), 9.14 (d, J = 1.2 Hz, 2H; H^3 or H^5), 9.24 (d, J = 1.5 Hz, 2H; H^3 or H^5), 9.64 ppm (s, 1H; H^2); ^{13}C NMR (50 MHz, CDCl_3 , 298 K): δ = 52.8, 111.7, 121.0, 121.3, 121.9, 124.4, 128.6, 131.0, 136.8, 137.5, 139.9, 149.4, 154.9, 155.1, 156.7, 163.5, 164.4, 165.7, 168.7 ppm; HR-FAB-MS: m/z calcd for $\text{C}_{34}\text{H}_{25}\text{N}_6\text{O}_4$: 581.193729; found: 581.193730 $[M^+ + \text{H}]$; IR (KBr): $\tilde{\nu}$ = 3065, 2955, 1732, 1560, 1543, 1364, 1254, 1231, 756, 734, 684, 665 cm^{-1} ; elemental analysis calcd (%) for $\text{C}_{34}\text{H}_{25}\text{N}_6\text{O}_4$: C 70.34, H 4.17, N 14.47; found: C 69.81, H 4.17, N 14.08.

4,6-Bis[6'-(pyrid-2'-yl)-4'-(thio-*n*-propyl)pyrid-2'-yl]-2-phenylpyrimidine (Ligand E): Ligand **E** was synthesized by using Potts' synthesis protocol (Scheme 4);^[24] the bis-Michael acceptor was synthesized according to the literature.^[25] 2-Acetylpyridine (0.43 g, 3.56 mmol) and the bis-Michael acceptor (1.00 g, 1.78 mmol) in THF (50 mL) were added to a stirred solution of potassium *tert*-butoxide (0.80 g, 7.12 mmol) in THF (30 mL) under Ar. The resulting red solution was stirred at room temperature for



Scheme 4. i) *t*BuOK, THF, RT; ii) NH_4OAc , AcOH.

16 h. Glacial acetic acid (10 mL) and ammonium acetate (5 g) were added. The mixture was heated under reflux for 2 h, cooled, and poured into water (200 mL), and the product was extracted with chloroform. The combined organic phases were washed with sat. NaHCO_3 and water, and dried over Na_2SO_4 ; the solvent was evaporated. The product was isolated by column chromatography (alumina, chloroform) as an off-white solid that was recrystallized from acetone to afford **E** (0.50 g, 0.81 mmol) as a white powder in 45% yield. ^1H NMR (200 MHz, CDCl_3 , 298 K): δ = 1.17 (t, J = 7.3 Hz, 6H), 1.87 (sext, J = 7.3 Hz, 4H), 3.18 (t, J = 7.3 Hz, 4H), 7.33 (dt, J = 7.6, 1.5 Hz, 2H), 7.57 (m, 3H), 7.82 (dt, J = 7.6, 1.5 Hz, 2H), 8.40 (d, J = 1.5 Hz, 2H), 8.52 (d, J = 1.5 Hz, 2H), 8.70 (m, 6H), 9.54 ppm (s, 1H); ^{13}C NMR (50 MHz, CDCl_3 , 298 K): δ = 13.7, 22.2, 32.9, 118.5, 118.8, 121.5, 124.0, 128.4, 128.6, 136.6, 149.2, 152.0, 155.1, 155.8, 163.9 ppm; elemental analysis calcd (%) for $\text{C}_{36}\text{H}_{32}\text{N}_6\text{S}_2$: C 70.56, H 5.26, N 13.71, S 10.47; found: C 70.25, H 5.22, N 13.64, S 10.18.

Complexes: The synthesis of complexes **1**,^[9a] **2**,^[9b] **6**,^[10b] and **7**^[9b] was carried out following literature protocols. A typical protocol for the synthesis of complexes **3**, **4**, **5**, and **8** is as follows: A suspension of the ligand (19.8 μmol) and the metal salt (19.8 μmol) in ACN (1.5 mL) was briefly heated until the mixture was dissolved completely. The solution was stirred for additional 12 h at room temperature (in the case of solubility problems under reflux). The complex was isolated by evaporation of the solvent or addition of diisopropyl ether (5 mL) to the solution until a precipitate formed. The precipitate was collected, washed with diisopropyl ether, and dried *in vacuo*. The crude product was used directly for the measurements without further purification.

Complex 3: ^1H NMR (200 MHz, $[\text{D}_3]\text{ACN}$, 298 K): δ = -98.1, -97.3, -27.1, -14.6, 0.2, 7.8, 11.7, 50.8, 53.5, 65.6, 122.4, 154.4, 235.3 ppm; FAB-MS: m/z : 3079.6 $[M^+ - 2\text{BF}_4]$, 2992.6 $[M^+ - 3\text{BF}_4]$, 2905.7 $[M^+ - 4\text{BF}_4]$, 2818.7 $[M^+ - 5\text{BF}_4]$, 1496.3 $[M^{2+} - 3\text{BF}_4]$, 1452.8 $[M^{2+} - 4\text{BF}_4]$, 1409.3 $[M^{2+} - 5\text{BF}_4]$; elemental analysis calcd (%) for $\text{C}_{112}\text{H}_{80}\text{N}_{24}\text{O}_{16}\text{Co}_4\text{B}_8\text{F}_{32}$: C 45.35, H 2.73, N 11.45; found: C 45.62, H 2.79, N 11.22.

Complex 4: ^1H NMR (200 MHz, $[\text{D}_3]\text{ACN}$, 298 K): δ = 0.5, 8.3, 42.0, 62.7, 63.8, 82.5, 117.3, 151.0 ppm; FAB-MS: m/z : 2774.4 $[M^+ - 2\text{BF}_4]$, 2687.6 $[M^+ - 3\text{BF}_4]$, 2601.0 $[M^+ - 4\text{BF}_4]$, 2514.4 $[M^+ - 5\text{BF}_4]$; elemental analysis calcd (%) for $\text{C}_{136}\text{H}_{96}\text{N}_{24}\text{O}_{16}\text{Co}_4\text{B}_8\text{F}_{32}$: C 53.59, H 3.17, N 11.07; found: C 50.01, H 3.07, N 10.57.

Complex 5: ^1H NMR (200 MHz, $[\text{D}_3]\text{ACN}$, 298 K): δ = -19.3, 1.9, 3.5, 8.0, 10.2, 13.1, 13.3, 21.5, 22.3, 40.6, 51.5, 73.7, 140.9, 167.6 ppm; FAB-MS: m/z : 3208.5 $[M^+ - 2\text{BF}_4]$, 3121.5 $[M^+ - 3\text{BF}_4]$, 3033.6 $[M^+ - 4\text{BF}_4]$, 2946.6 $[M^+ - 5\text{BF}_4]$, 1560.3 $[M^{2+} - 3\text{BF}_4]$, 1516.8 $[M^{2+} - 4\text{BF}_4]$, 1473.3 $[M^{2+} - 5\text{BF}_4]$; elemental analysis calcd (%) for $\text{C}_{144}\text{H}_{128}\text{N}_{24}\text{S}_8\text{Co}_4\text{P}_8\text{F}_{32}$: C 50.45, H 3.87, N 10.08; found: C 50.04, H 3.50, N 9.71.

Complex 8: ^1H NMR (200 MHz, $[\text{D}_3]$ nitromethane, 298 K): δ = 1.32 (br), 8.5 ppm (br); FAB-MS: m/z : 2673.9 $[M^+ - 2\text{ClO}_4]$, 2574.8 $[M^+ - 3\text{ClO}_4]$, 2474 $[M^+ - 4\text{ClO}_4]$, 2376.9 $[M^+ - 5\text{ClO}_4]$, 1286.9 $[M^{2+} - 5\text{BF}_4]^{2+}$; elemental analysis calcd (%) for $\text{C}_{120}\text{H}_{80}\text{N}_{24}\text{Cl}_8\text{Mn}_4\text{O}_{32}$: C 50.15, H 3.81, N 11.69; found: C 50.24, H 2.98, N 12.39.

Acknowledgement

We thank Dr. R. G. Khoury for samples of intermediates for the synthesis of ligand **C**. A post-doctoral scholarship provided by "Deutscher Akademischer Austauschdienst" (DAAD) (M.R.) and financial support from the "Ministère de l'Éducation Nationale, de la Recherche et de la Technologie" are gratefully acknowledged (E.B.).

- [1] R. Compano, L. Molenkamp, D. J. Paul, Technology Roadmap for Nanoelectronics, European Commission IST Programme: Future and Emerging Technologies, Microelectronics Advanced Research Initiative; <http://nanoworld.org/nanolibrary/nanoroad.pdf>
- [2] a) A. Bachtold, P. Hadley, T. Nakanishi, C. Dekker, *Science* **2001**, *294*, 1317–1320; b) P. G. Collins, M. S. Arnould, P. Avouris, *Science* **2001**, *292*, 706–710.
- [3] a) Y. Huang, X. Duan, Y. Ciu, L. J. Lauhon, K.-H. Kim, C. M. Lieber, *Science* **2001**, *294*, 1313–1316; b) A. Bachtold, P. Hadley, T. Nakanishi, C. Dekker, *Science* **2001**, *294*, 1317–1320.

- [4] a) C. P. Collier, G. Mattersteig, E. W. Wong, Y. Luo, J. Sampaio, F. M. Raymo, J. M. Stoddart, J. R. Heath, *Science* **1999**, *285*, 391–395; b) C. P. Collier, G. Mattersteig, E. W. Wong, Y. Luo, K. Beverly, F. M. Raymo, J. F. Stoddart, J. R. Heath, *Science* **2000**, *289*, 1172–1176.
- [5] a) J.-M. Lehn, “*Supramolecular Chemistry: Concepts and Perspectives*”, VCH, Weinheim, Chapters 8 and 9, **1995**; b) J.-M. Lehn, *Science*, **2002**, *295*, 2400–2403.
- [6] a) V. Balzani, F. Scandola in *Comprehensive Supramolecular Chemistry*, Vol. 10, (Eds.: J. L. Atwood, J. E. D. Davies, D. D. MacNicol, F. Vögtle, J.-M. Lehn) Elsevier, Oxford, **1996**, pp. 687–730; b) V. Balzani, F. Scandola, *Supramolecular Photochemistry*, Ellis Harwood, Chichester **1991**; c) V. Balzani, A. Credi, F. M. Raymo, J. F. Stoddart, *Angew. Chem.* **2000**, *112*, 3484–3530; *Angew. Chem. Int. Ed.* **2000**, *39*, 3348–3391.
- [7] A. Vlcek, Jr. in *Electron Transfer in Chemistry*, Vol. 2 (Ed.: V. Balzani), Wiley-VCH, Weinheim **2001**, 804–877.
- [8] a) C. M. Elliot, E. J. Hershenhart, *J. Am. Chem. Soc.* **1982**, *104*, 7519–7526; b) Y. Ohsawa, M. K. DeArmond, K. W. Hanck, D. E. Morris, D. G. Whitten, P. E. Neveux, Jr., *J. Am. Chem. Soc.* **1983**, *105*, 6522–6524; c) M. Krejciak, A. A. Vlcek, *Inorg. Chem.* **1992**, *31*, 2390–2395; d) M. Marcaccio, F. Paolucci, C. Paradisi, S. Roffia, C. Fontanesi, L. J. Yellowlees, S. Serroni, S. Campagna, G. Denti, V. Balzani, *J. Am. Chem. Soc.* **1999**, *121*, 10081–10091; E. Perez-Cordero, R. Buigas, N. Brady, L. Echegoyen, C. Arana, J.-M. Lehn, *Helv. Chim. Acta* **1999**, *77*, 1222–1228.
- [9] a) G. S. Hanan, D. Volkmer, U. S. Schubert, J.-M. Lehn, G. Baum, D. Fenske, *Angew. Chem.* **1997**, *109*, 1929–1931; *Angew. Chem. Int. Ed. Engl.* **1997**, *36*, 1842–1844; b) J. Rojo, F. J. Romero-Salguero, J.-M. Lehn, G. Baum, D. Fenske, *Eur. J. Inorg. Chem.* **1999**, 1421–1428.
- [10] a) O. Waldmann, J. Hassmann, P. Müller, G. S. Hanan, D. Volkmer, U. S. Schubert, J.-M. Lehn, *Phys. Rev. Lett.* **1997**, *78*, 3390–3393; b) E. Breuning, M. Ruben, J.-M. Lehn, F. Renz, Y. Garcia, V. Ksenofontov, P. Gütllich, E. Wegelius, K. Rissanen, *Angew. Chem.* **2000**, *112*, 4312–4315; *Angew. Chem. Int. Ed.* **2000**, *14*, 2504–2507.
- [11] M. Ruben, E. Breuning, J.-P. Gisselbrecht, J.-M. Lehn, *Angew. Chem.* **2000**, *112*, 2563–2566; *Angew. Chem. Int. Ed.* **2000**, *39*, 4139–4142.
- [12] M.-T. Youinou, N. Rahmouni, J. Fischer, J. A. Osborn, *Angew. Chem.* **1992**, *104*, 771–773; *Angew. Chem. Int. Ed. Engl.* **1992**, *31*, 733–736.
- [13] C. Dietrich-Buchecker, J.-P. Sauvage, J. M. Kern, *J. Am. Chem. Soc.* **1989**, *111*, 7791–7800.
- [14] a) C. B. Gorman, *Adv. Mater.* **1997**, *9*, 1117–1119; b) P. J. Dandliker, F. Diederich, J.-P. Gisselbrecht, A. Louati, M. Gross, *Angew. Chem.* **1995**, *107*, 2906–2909; *Angew. Chem. Int. Ed. Engl.* **1995**, *34*, 2725–2728; c) C. M. Cardona, S. Mendoza, A. A. Kaifer, *Chem. Soc. Rev.* **2000**, *29*, 37–42.
- [15] C. Hensch, A. Leo, R. W. Taft, *Chem. Rev.* **1991**, *91*, 165–195.
- [16] a) L. Echegoyen, L. E. Echegoyen, *Acc. Chem. Res.* **1998**, *31*, 593–601; b) Q. Xien, E. Pérez-Cordero, L. Echegoyen, *J. Am. Chem. Soc.* **1992**, *114*, 3978–3980; c) P.-M. Allemand, A. Koch, F. Wudl, Y. Rubin, F. Diederich, M. M. Alvarez, S. J. Anz, R. L. Whetten, *J. Am. Chem. Soc.* **1991**, *113*, 1050–1051; d) T. Suzuki, K. Kikuchi, F. Oguri, Y. Nakao, S. Suzuki, Y. Achiba, K. Yamamoto, H. Fuasaka, T. Takahashi, *Tetrahedron* **1996**, *52*, 4973–4982; e) J. Li, C. Papadopoulos, J. Xu, *Nature* **1999**, *402*, 253–254.
- [17] J. M. Rao, M. C. Hughes, D. J. Macero, *Inorg. Chim. Acta* **1976**, *16*, 231–236.
- [18] P. S. Braterman, J. I. Songh, R. Peacock, *Inorg. Chem.* **1992**, *31*, 555–559;
- [19] A. A. Vlcek, *Coord. Chem. Rev.* **1982**, *43*, 39–62.
- [20] a) B. S. Brunschwigg, N. Sutin, *Coord. Chem. Rev.* **1999**, *133*, 273–295; b) J. A. McCleverty, M. D. Ward, *Acc. Chem. Res.* **1998**, *31*, 842–865; c) F. Barigelletti, L. Flamini, V. Balzani, J.-P. Collin, J.-P. Sauvage, A. Sour, E. C. Constable, A. M. W. Cargill Thompson, *J. Am. Chem. Soc.* **1994**, *116*, 7692–7699; d) J.-P. Sauvage, J.-P. Collin, J.-C. Chambron, S. Guillerez, C. Coudret, V. Balzani, F. Barigelletti, L. De Cola, L. Flamigni, *Chem. Rev.* **1994**, *94*, 993–1016; e) G. Giuffrida, S. Campagna, *Coord. Chem. Rev.* **1994**, *135/136*, 517–525.
- [21] a) G. A. Heath, L. J. Yellowlees, P. S. Braterman, *J. Chem. Soc. Chem. Commun.* **1981**, 287–289; b) P. S. Braterman, J.-I. Song, *J. Org. Chem.* **1991**, *56*, 4678–4682.
- [22] G. S. Hanan, Ph.D. Thesis, Université Louis Pasteur Strasbourg (France), **1995**.
- [23] C. Bolm, M. Erwald, M. Felder, G. Schingloff, *Chem. Ber.* **1992**, *125*, 1169–1178.
- [24] a) K. T. Potts, *Bull. Soc. Chim. Belg.* **1990**, *99*, 741–768; b) K. T. Potts, K. A. Gheysen Raiford, M. Keshavarz, *J. Am. Chem. Soc.* **1993**, *115*, 2793–2807.
- [25] K. M. Gardinier, R. G. Khoury, J.-M. Lehn, *Chem. Eur. J.* **2000**, *22*, 4124–4131.

Received: August 16, 2002 [F4350]